Electronic Supplementary Information for Chemical Science

A Novel Synergistic Enhanced Chemiluminescence Achieved by Multiplex Nanoprobe for Biological Applications Combined with Dual-Amplification of Magnetic Nanoparticles

Sai Bi, Hong Zhou and Shusheng Zhang*

State Key Laboratory Base of Eco-chemical Engineering，College of Chemistry and Molecular Engineering，Qingdao University of Science and Technology，Qingdao 266042，P.R.China.

* Corresponding author. Tel.: +86-532-84022750; Fax: +86-532-84022750

E-mail: shushzhang@126.com

Additionally experimental section

Apparatus

A FI-CL instrument (MPI-F, Remex Analytical Instrument Co. Ltd., Xi'an, China), including a model IFIS-D flow injection system, a model RFL-1 luminometer, and a computer was used to perform the CL. Transmission electron microscopy (TEM) images were carried out with a JEM-2000EX/ASID2 (HITACHI, Japan). A CARY 500 Scan UV/Vis-NIR spectrophotometer (Varian, USA) was used to record the UV-vis absorption spectra. Fe_3O_4-Au core-shell magnetic nanoparticles (Fe_3O_4@Au) (~50 nm, 5 mg mL^{-1}) was purchased from Shaanxi Lifegen Co., Ltd. Carboxyl groups modified magnetic nanoparticles (~500 nm, 10 mg mL^{-1}) and magnetic rack were obtained from BaseLine ChromTech Research Centre (Tianjin, China).

Reagents

All the DNA sequences were synthesized and purified by SBS Genetech Co. Ltd. (China), and the sequences of this work are listed in **Table S1**. 1-Ethyl-3-(3-dimethylaminopropyl)-carbodiimide hydrochloride (EDC), and imidazole were obtained from Sigma. Tri(2-carboxyethyl)phosphine hydrochloride (TCEP, 98%) was purchased from Alfa Aesar (Massachusetts). A luminol (standard powder, Sigma-Aldrich) stock solution (1.0×10^{-2} M) was prepared by dissolution in 0.1 M NaOH and further stored in dark. The stock solution was consecutively diluted with 0.1 M $Na_2B_4O_7$-NaOH in order to obtain the proper solution used for CL determination.

Cancer cell culture

Ramos cells as target cells and CEM cells as control cells were separately cultured in cell flasks according to the instructions from the American Type Culture Collection. The cell line was grown to 90% confluence in RPMI 1640 medium supplemented with 10% (v/v) fetal bovine serum (FBS) and 100 IU mL^{-1} penicillin-streptomycin at 37 ^{o}C, and the cells were cultured in a humidified atmoshpere with 5% CO_2. The cell density was determined using a hemocytomer prior to each experiment. And then, a 3.0 mL suspension of ~1.0×10^6 cells dispersed in RPMI 1640 cell media buffer was centrifuged at 3000 rpm for 5 min and washed with phosphate-buffered saline (18.6 mM phosphate, 4.2 mM KCl, and 154.0 mM NaCl) five times and resuspended in 1.0 mL cell media buffer.

Bacteria culture and DNA extraction and isolation

The baterial strain used was *E. coli* uidA which were cultured in cell flasks according to the instructions of the American Type Cell Culture. The pure culture was grown in a model G25 incubator shaker (P.A.C.I.S.A., New Brunswick Scientific Co. Inc. Edison, NJ) at 37 ^{o}C overnight before the bacterial concentration was determined by the conventional surface plate counting method. The genomic DNA was isolated by using a Bacteria Genomic DNA Isolation Kit (Sangon, Shanghai). A 120- and 250-bp in the genomic DNA fragment were chosen to be amplified, respectively, containing the target sequence (36-mer) for the DNA hybridizaiotn detection. Asymmetric PCR amplification was conducted in a Bio-Rad PCR cycler (PTC-100) in order to ensured that the product was in the single-stranded format that could be directly detected.[3-6] The 100 μL of PCR reaction mixture contained 5 μL of *E. coli* uidA genomic DNA extract (150 ng μL^{-1}), a pair of asymmetric primers (primer 1/primer 3 = 100:1 for 120-bp region, primer2/primer 3 = 100:1 for 250-bp region), and other components following the protocol for PCR with *Taq* DNA ploymerase. The amplification protocol was performed at 94 ^{o}C for 10 min for denaturation followed by 30 cycles of 94 ^{o}C for 30 s (denaturation), 51 ^{o}C for 30 s (annealing), and 72 ^{o}C for 60 s (extension). The reaction system was further incubated for 10 min at 72 ^{o}C to extend any incomplete products. The PCR products were diluted by 10 times and then subjected to FI-CL detection as described above.

Table S1 DNA sequence used in this work

No	oligonucleotides name	sequences	description
1	aptamer	5'-NH_2-TAC AGA ACA CCG GGA GGA TAG TTC GGT GGC TGT TCA GGG TCT CCT CCC GGT G-3'	specific recognition of Romas cell
2	random DNA	5'-NH_2-ATG TCT TGT GGC CCT CCT ATC AAG CCA CCG ACA AGT CCC ACT CCT CCC GGT G-3'	nonspecific recognition of Romas cell
3	target DNA (t-DNA)	5'-GCC GCT CAC ACG ATA CCT AAT GTG CAC CGG GAG GAG-3'	complementary to aptamer with 12-mer, and c-DNA and p2-DNA
4	capture DNA (biotin-c-DNA)	5'-biotin-CTC CTC CCG GTG CAC-3'	biotin modified capture DNA immobilized on streptavidin-coated substrate
5	first-probe DNA (p1-DNA)	5'-TAT CGT GTG AGC GGC TTT TTT-NH_2-3'	amino group modified probe DNA coated on MNPs and complementary to t-DNA
6	bio-bar-code DNA (bbc-DNA)	5'-GCT CAT ATG GAC CTC TTT TTT-NH_2-3'	amino group modified probe DNA coated on MNPs and noncomplementary to p1-DNA
7	second-probe DNA (p2-DNA)	(1) 5'-NH_2-AAA GCC GCT CAC ACG ATA- SH-3' (2) 5'-NH_2-AAA GAG GTC CAT ATG AGC- SH-3'	(1) thiol and amino group modified probe DNA complementary to p1-DNA to fabricate CuS-p2-Au (2) thiol and amino group modified probe DNA complementary to bbc-DNA to fabricate CuS-p2-Au
8	primer 1 (5')	5'-GCG AAA ACT GTG GAA TTG AT-3'	
9	primer 2 (5')	5'-GTA TCA GCG CGA AGT CTT TA-3'	primers used for asymmetric PCR
10	primer 3 (3')	5'-TGA TGC TCC ATC ACT TCC TG-3'	
11	250-bp target	5'-GCG AAA ACT GTG GAA TTG ATC AGC GTT GGT GGG AAA GCG CGT TAC AAG AAA GCC GGG CAA TTG CTG TGC CAG GCA GTT TTA ACG ATC AGT TCG CCG ATG CAG ATA TTC GTA ATT ATG CGG GCA ACG TCT GGT ATC AGC GCG AAG TCT TTA TAC CGA AAG GTT GGG CAG GCC AGC GTA TCG TGC TGC GTT TCG ATG CGG TCA CTC ATT ACG GCA AAG TGT GGG TCA ATA ATC AGG AAG TGA TGG AGC ATC A-3'	uidA gene of *E. Coli* used for the detection of DNA hybridization. The highlight in yellow are the target DNA sequences of 250- and 120-bp by asymmetric PCR
12	120-bp target	5'-GTA TCA GCG CGA AGT CTT TAT ACC GAA AGG TTG GGC AGG CCA GCG TAT CGT GCT GCG TTT CGA TGC GGT CAC TCA TTA CGG CAA AGT GTG GGT CAA TAA TCA GGA AGT GAT GGA GCA TCA-3'	
13	DNA sequences used for uidA gene of *E. Coli* hybridization detection		
14	biotin-c-DNA	5'-biotin-TAA TGA GTG ACC GCA-3'	
15	p1-DNA	5'-CGC AGC ACG ATA CGC TTT TTT- NH_2-3'	
16	p2-DNA	(1) 5'-NH_2-AAA GCG TAT CGT GCT GCG- SH-3' (2) 5'-NH_2-AAA GAG GTC CAT ATG AGC- SH-3'	

DNA hybridization detection

DNA hybridization detection in luminol-H_2O_2-Cu^{2+} CL system.

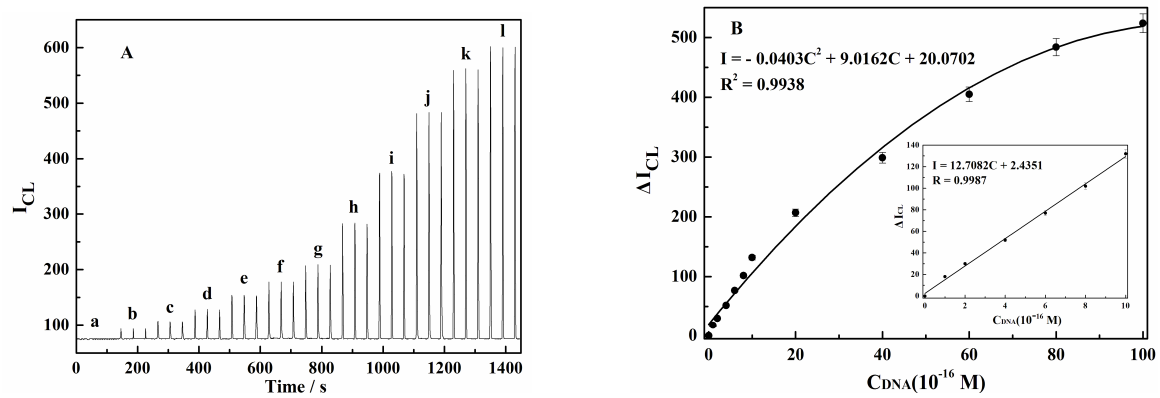

Fig. S1 (A) CL signals for Cu^{2+} dissolved from a series of CuS/p2-DNA/Au/MNPs conjugates corresponding to different concentrations of t-DNA. The concentrations of t-DNA: (a) 0; (b) 1.0×10^{-16}; (c) 2.0×10^{-16}; (d) 4.0×10^{-16}; (e) 6.0×10^{-16}; (f) 8.0×10^{-16}; (g) 1.0×10^{-15}; (h) 2.0×10^{-15}; (i) 4.0×10^{-15}; (j) 6.0×10^{-15}; (k) 8.0×10^{-15}; (l) 1.0×10^{-14} M. (B) The calibration curve of peak height versus the concentration of t-DNA from 1.0×10^{-16} to 1.0×10^{-14} M. Inset is the amplification of the linear range from 1.0×10^{-16} to 1.0×10^{-15} M for t-DNA determination.

DNA hybridization detection in luminol-H_2O_2-Fe^{3+} CL system.

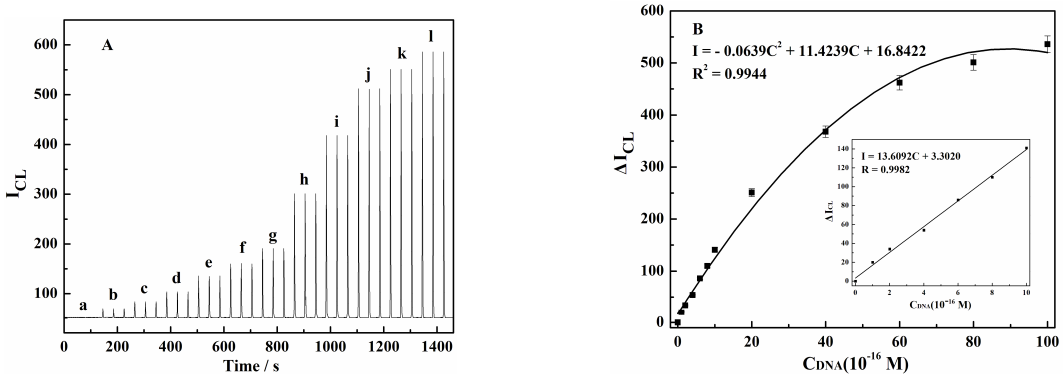

Fig. S2 (A) CL signals for Fe^{3+} dissolved from a series of CuS/p2-DNA/Au/MNPs conjugates corresponding to different concentrations of t-DNA. The concentrations of t-DNA: (a) 0; (b) 1.0×10^{-16}; (c) 2.0×10^{-16}; (d) 4.0×10^{-16}; (e) 6.0×10^{-16}; (f) 8.0×10^{-16}; (g) 1.0×10^{-15}; (h) 2.0×10^{-15}; (i) 4.0×10^{-15}; (j) 6.0×10^{-15}; (k) 8.0×10^{-15}; (l) 1.0×10^{-14} M. (B) The calibration curve of peak height versus the concentration of t-DNA from 1.0×10^{-16} to 1.0×10^{-14} M. Inset is the amplification of the linear range from 1.0×10^{-16} to 1.0×10^{-15} M for t-DNA determination.

DNA hybridization detection in luminol-H_2O_2-Cu^{2+}-Fe^{3+} SECL system.

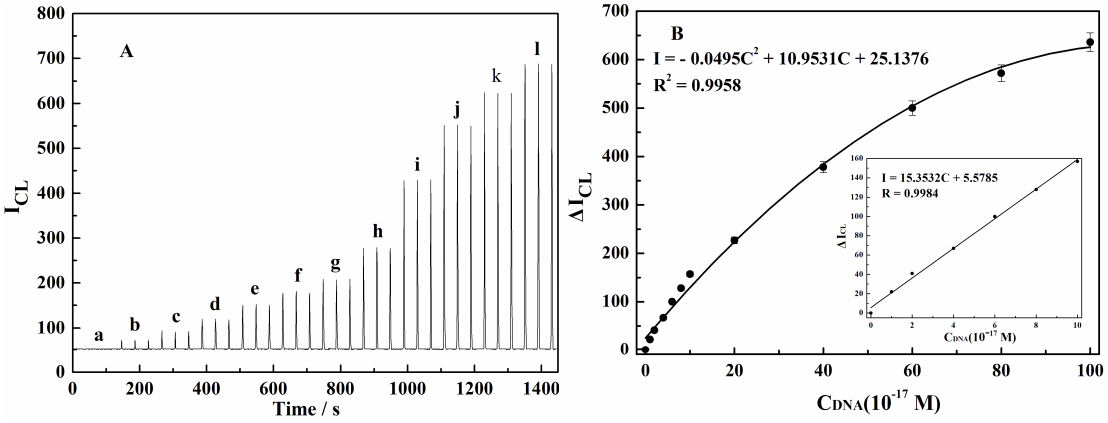

Fig. S3 (A) CL signals for Cu^{2+} and Fe^{3+} dissolved from a series of CuS/p2-DNA/Au/MNPs conjugates corresponding to different concentrations of t-DNA. The concentrations of t-DNA: (a) 0; (b) 1.0×10^{-17}; (c) 2.0×10^{-17}; (d) 4.0×10^{-17}; (e) 6.0×10^{-17}; (f) 8.0×10^{-17}; (g) 1.0×10^{-16}; (h) 2.0×10^{-16}; (i) 4.0×10^{-16}; (j) 6.0×10^{-16}; (k) 8.0×10^{-16}; (l) 1.0×10^{-15} M. (B) The calibration curve of peak height versus the concentration of t-DNA from 1.0×10^{-17} to 1.0×10^{-15} M. Inset is the amplification of the linear range from 1.0×10^{-17} to 1.0×10^{-16} M for t-DNA determination.

Table S2 Comparison between the proposed CL assay and other reported techniques for the detection of DNA hybridization[a]

format	label	techniques[c]	detection limit of ssDNA
nanoparticle and nanostructure -based methods for DNA hybridization	Au and CuS NPs[7]	CL	4.8 fM
	MNPs [8]	bio-bar-code amplified FI-CL	0.32 fM
	Au nanoparticles (cross-linked)[9]	colorimetric	~10 nM
	Au nanoparticles (cross-linked)[10]	electrochemical	100 fM
	Au NPs (non-cross-linked)[11]	colorimetric	60 nM
	Au NPs [12]	laser diffraction	~50 fM
	Au NPs [13]	SPR	10 pM
	Au NPs [14]	PSA	15 nM
	Au NPs [15]	chronocoulometric	10 fM
	Au NPs with Ag amplification[16, 17]	Scanometric	50 fM
	Au NPs with Ag amplification[18]	Raman spectroscopy	~20 fM
	Au NPs with Ag amplification[19]	electrical	500 fM
	Au NPs with Ag amplification[20]	PSA	32 pM
	silver NPs[21]	ASV	0.5 pM
	silver NPs[22]	CL	5 fM
	CuS NPs[23]	CL	550 fM
	ZnS, CdS, PbS NPs[24]	stripping voltammetry	270 pM
	ZnS and CdSe quantum dots[25]	fluorescence	2 nM
	Liposome[26]	liposome-amplified electrochemical	50 fM
	MNPs[27]	magnetically amplified electrochemical	0.5 fM
	MNPs[28]	PSA	0.1 fM
	Au NPs with Ag amplification[29]	bio-bar-code amplified scanometric	0.5 fM
	Au and CuS NPs [b]	daul-amplified FI-CL	72 aM
	MNPs, Au and CuS NPs [b]	daul-amplified FI-CL	6.8 aM

[a] Some were adapted from ref 17. [b] This method. [c] PSA, potentiometric stripping analysis; ASV, anodic stripping voltammetry; SPR, surface Plasmon resonance; FI-CL, flow-injection chemiluminescence.

Selectivity of the DNA biosensor

The selectivity of the present strategy was investigated by luminol-H_2O_2-Cu^{2+}-Fe^3 to hybridized with 8.0×10^{-16} M of complete complementary t-DNA sequences, the two-base mismatched DNA sequences and the noncomplementary sequences, respectively. The CL kinetic curves can be seen in **Fig. S4**. A well-defined CL signal of luminol-H_2O_2-Cu^{2+}-Fe^{3+} was obtained for the complementary sequences. The CL intensity for two-base mismatched sequences was significantly weaker than that of the complementary sequences, and the noncomplementary sequences showed no response.

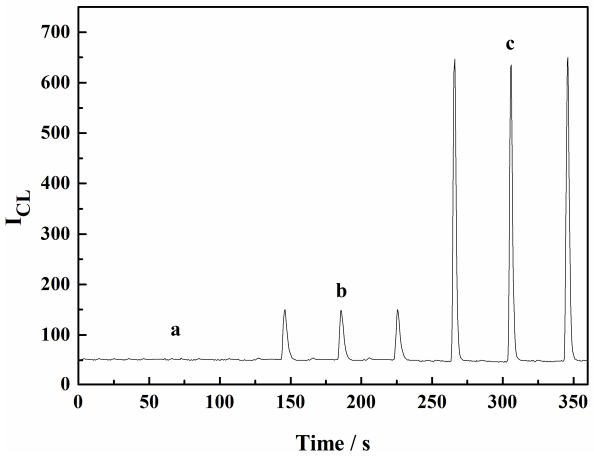

Fig. S4 FI-CL signals of luminol-H_2O_2 catalyzed by Cu^{2+} and Fe^{3+} dissolved from CuS/p2-DNA/Au/MNPs hybridized with different target DNA. (a) Noncomplementary sequences; (b) two-base mismatched sequences; (c) complementary sequences. All the concentrations of t-DNA are 8.0×10^{-16} M.

Detection of PCR Products

Confirmation of asymmetric PCR amplification using gel electrophoresis

In order to test the real applicability of the developed method, asymmetric PCR was used to amplify a 120- and 250-bp DNA fragment containing the target sequence (36-mer) for the direct hybridization detection. What is noteworthy is that while the asymmetric PCR is usually much less efficient in amplification than normal PCR due to the fact that the depletion of one primer will lead to a linear, nonexponential, amplificaiton region, it generates DNA target in the single-stranded format that avoids the denaturing step during subsequent probe-target hybridization. The results obtained in the screening of the asymmetric PCR products by gel electrophoresis are shown in **Fig. S5A** in the main text. From left to right, the DNA size marker, asymmetric PCR product using genomic DNA from *E. coli*, for a concentration of 1.0×10^{-7} M. Electrophoresis confirmed the successful amplification of PCR products with the right size (120 and 250

bp).

FI-CL detection of PCR amplicons using genomic DNA as template

The PCR samples were diluted to the desired concentration using 50 mM PBS buffer solution (pH 7.4) and directly applied for the daul-amplification FI-CL detection. Thus, the desired amount of PCR product was used for each test following the same procedure used for synthetic olilgonucleotides. Satisfactorily, our strategy performed equally well with 120 and 250 bp PCR products despite the fact that these targets were much longer than the model system described above. It was found that by coupling asymmetric PCR, as low as 1.0×10^{-16} M *E. coli* genomic DNA (250 bp) can be detected (**Fig. S5B**), which suggested that the MNP daul-amplification method was a promising technology for the rapid detection of *E. coli*.

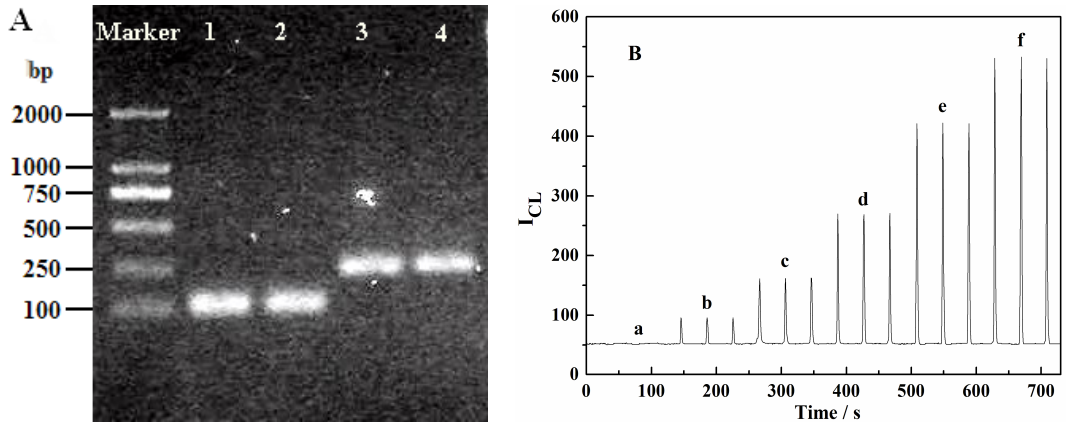

Fig. S5 (A) Gel electrophoresis detection of *E.coli* uidA gene asymmetric PCR products. Lanes 1 and 2, 120-bp asymmetric product (uidA) using genomic DNA from *E. coli*; lanes 3 and 4, 250-bp asymmetric product (uidA) using genomic DNA from *E. coli*. (B) Concentration profile for the detection of *E. coli* genomic DNA (250 bp) based on the MNPs dual-amplification FI-CL detection of luminol-H_2O_2-Cu^{2+}-Fe^{3+} system coupled with an asymmetric PCR protocol. The DNA template was the genomic DNA isolated from *E. coli* and stepwisely diluted to the required concentration: (a) 0; (b) 1.0×10^{-16}; (c) 5.0×10^{-16}; (d) 1.0×10^{-15}; (e) 5.0×10^{-15}; (f) 1.0×10^{-14} M.

Investigation of luminol-H_2O_2-Cu^{2+}-Fe^{3+} synergistic CL reaction system

First, the effects of concentration of Cu^{2+} and Fe^{3+} standard solution were investigated, respectively. The catalyzed CL intensity was found to be linear with the concentration of Cu^{2+} or Fe^{3+}. As shown in **Fig. S6**, the concentration of 1.0×10^{-9} to 1.0×10^{-8} g mL^{-1} for Cu^{2+} and 1.0×10^{-10} to 1.0×10^{-9} g mL^{-1} for Fe^{3+} could be expressed as the linear regression equation of Y = 14.2713X + 3.2270 (X is the concentration of Cu^{2+}, 10^{-9} g mL^{-1}; Y is the CL intensity, n = 7, R = 0.9983), and Y = 20.1553X + 6.3123 (X is the concentration of Fe^{3+}, 10^{-10} g mL^{-1}; Y is the CL intensity, n = 7, R = 0.9988), respectively.

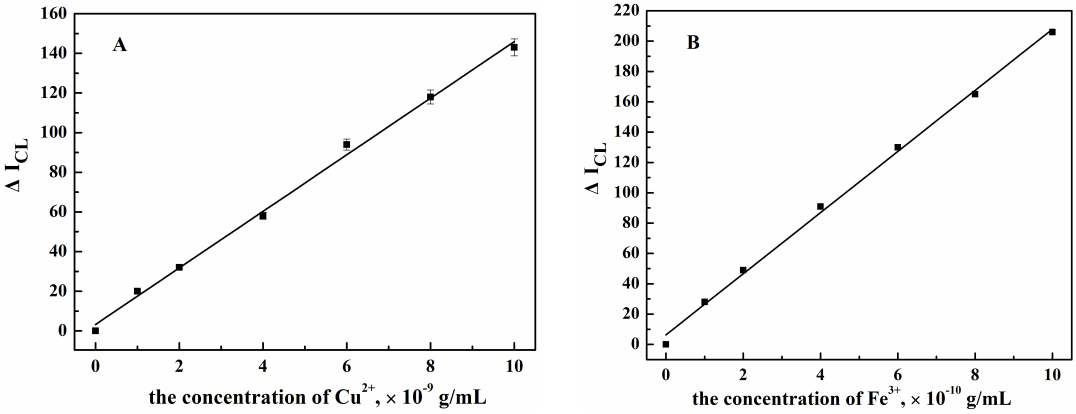

Figure S6. CL signal calibration curves of (A) Cu^{2+} and (B) Fe^{3+} standard solution.

The ratio of Fe^{3+} and Cu^{2+} dissolved from CuS/p2-DNA/Au/MNPs conjugates was determined by both detecting 1.0×10^{-15} M t-DNA and calculated based on the calibration curves of Cu^{2+} and Fe^{3+} standard solution. For example, 1.0×10^{-15} M t-DNA was detected at step IV (**Scheme 1** in the main text) in luminol-H_2O_2-Fe^{3+} CL system by dissolving dehybridized MNPs into Fe^{3+}, which achieved a CL intensity of 191. From the calibration curve of Fe^{3+} standard solution, the corresponding concentration of 6.7×10^{-10} g mL^{-1} Fe^{3+} was obtained. In the same way, a concentration of 9.1×10^{-9} g mL^{-1} Cu^{2+} could be determined. Thus, the mass concentration ratio of Fe^{3+} and Cu^{2+} dissolved from CuS/p2-DNA/Au/MNPs conjugates was 6.7×10^{-10}/ 9.1×10^{-9} = 1: 14. The results are summarized in **Table S3**.

Table S3 Determination of the ratio of Fe^{3+} and Cu^{2+} dissolved from Au-p2-CuS-MNPs conjugates

t-DNA (M)	I_{CL} (Fe^{3+})	[Fe^{3+}] (g mL^{-1})	I_{CL} (Cu^{2+})	[Cu^{2+}] (g mL^{-1})	[Fe^{3+}]/[Cu^{2+}]
1.0×10^{-15}	191	6.7×10^{-10}	182	9.1×10^{-9}	1:14

Subsequently, the luminol-H_2O_2-Cu^{2+}-Fe^{3+} synergistic CL reaction system was investigated at Fe^{3+}/Cu^{2+} ratio of 1:14. The abscissa of **Fig. S7** was shown the concentration of Fe^{3+}, the concentration of Cu^{2+} was 14 fold of Fe^{3+} in the mixture solution. A linear range of 1.0×10^{-11} to 1.0×10^{-10} g mL^{-1} for Fe^{3+} and 1.4 ×

10^{-10} to 1.4×10^{-9} g mL^{-1} for Cu^{2+} of the mixture was achieved which was significantly improved compared to monometallic Fe^{3+} or Cu^{2+} catalysts for luminol-H_2O_2 CL system.

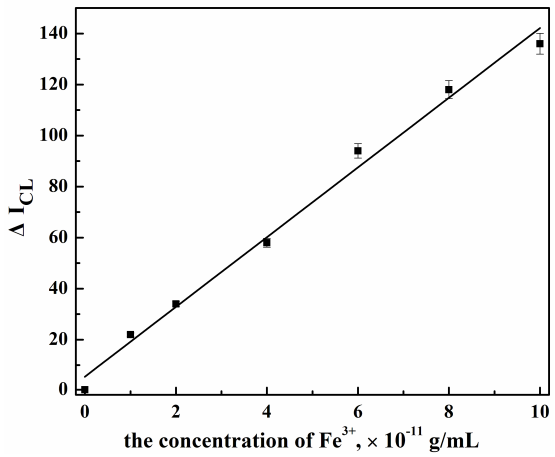

Fig. S7 CL signal calibration curves of Fe^{3+} and Cu^{2+} mixture solution at the ratio of Fe^{3+}/Cu^{2+} at 1:14.

Mechanism of the luminol-H_2O_2 catalyzed by cupric and ferric Ions

In order to reason the mechanism of luminol-H_2O_2-Cu^{2+}-Fe^{3+} synergistic CL reaction system, The UV-visible absorption spectra and fluorescence spectra of different systems were investigated (**Fig. S8**). From **Fig. S8A**, the absorption spectra of luminol, luminol-H_2O_2, luminol-Cu^{2+}, luminol-Fe^{3+}, luminol-Cu^{2+}-Fe^{3+}, luminol-H_2O_2-Cu^{2+}, luminol-H_2O_2-Fe^{3+} and luminol-H_2O_2-Cu^{2+}-Fe^{3+} appeared quite similar. From **Fig. S8B**, the fluorescence spectra of luminol-H_2O_2-Cu^{2+}-Fe^{3+} kept almost the same as luminol-H_2O_2. Thus, it could be proposed that no coordination complex was formed in the research conditions, and the possible CL mechanism of luminol-H_2O_2-Cu^{2+}-Fe^{3+} system was not the "coordination complex mechanism". The presumptive "free readical mechamisn" was discussed in the main text.

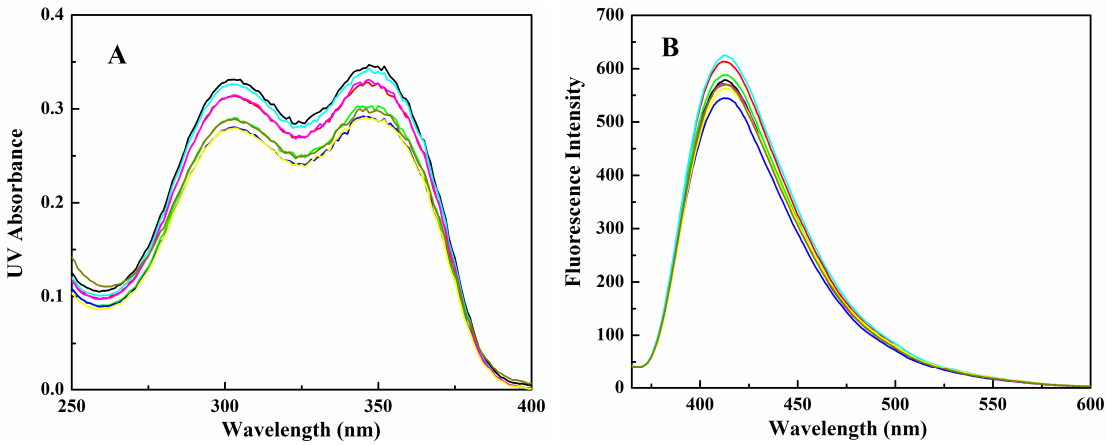

Fig. S8 (A) The UV absorption spectra of luminol (black), luminol-H_2O_2 (red), luminol-Fe^{3+} (green), luminol-Cu^{2+} (blue), luminol-Cu^{2+}-Fe^{3+} (cyan), luminol-H_2O_2-Fe^{3+} (magenta), luminol-H_2O_2-Cu^{2+} (yellow),

and luminol-H_2O_2-Cu^{2+}-Fe^{3+} (dark yellow). (B) Fluorescence spectra of luminol (black), luminol-Cu^{2+} (red), luminol-Fe^{3+} (green), luminol-Cu^{2+}-Fe^{3+} (blue), luminol-H_2O_2 (cyan), luminol-H_2O_2-Cu^{2+} (magenta), luminol-H_2O_2-Fe^{3+} (yellow), and luminol-H_2O_2-Cu^{2+}-Fe^{3+} (dark yellow). The concentrations of luminol and H_2O_2 were 5.0×10^{-5} M and 2.0×10^{-4} M, respectively. The concentrations of Fe^{3+} and Cu^{2+} standard solution used in this mechanism investigation were 1.0×10^{-8} and 1.4×10^{-7} M, respectively.

Determination of the amounts of t-aptamer-Fe_3O_4@Au used for cell assays

The amounts of t-DNA/aptamer/Fe_3O_4@Au used was carefully selected to allow saturation of the highest number of cells while using the minimum amounts of nanoparticles to reduce the cost and background of the solution, thus facilitating an easier detection of the lower end of the cell concentration. As seen in **Fig. S9**, with increasing amounts of t-DNA/aptamer/Fe_3O_4@Au with 10000 target Ramos cells, the CL intensities of luminol-H_2O_2-Cu^{2+}-Fe^{3+} were increased systematically and reached a plateau at 50 μL of t-DNA/aptamer/Fe_3O_4@Au. In addition, the CEM control cells did not induce any significant changes in the CL signal as compared to that of the target cells and there was no significant difference between the samples regardless of the increase amounts of the t-DNA/aptamer/Fe_3O_4@Au. This indicated that the target cells can be preferentially extracted from a sample, while hardly any of the CEM cells were extracted using the same method. Since the use of 50 μL of t-DNA/aptamer/Fe_3O_4@Au had a high CL intensity, this amount had used for sample assay experiments to allow for binding of both nanoparticles types to the same cell. The results indicated that the Fe_3O_4@Au were both selective for the target cells by discriminating against the control cells.

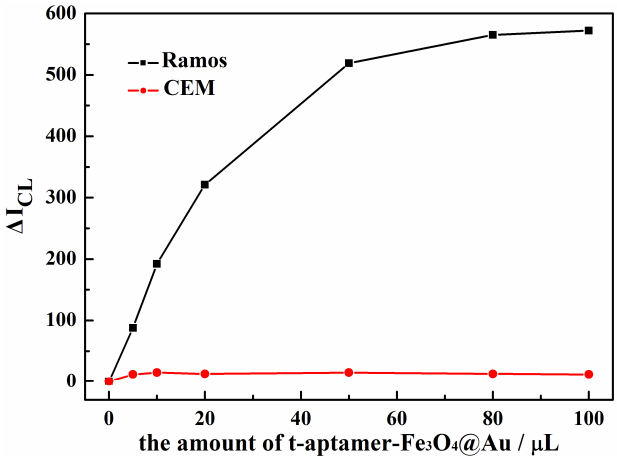

Fig. S9 Luminol-H_2O_2-Cu^{2+}-Fe^{3+} SECL determination of the amounts of t-DNA/aptamer/Fe_3O_4@Au between Ramos target cells and CEM control cells.

Table S4 Comparison between the proposed FI-CL assay and other reported techniques for cells detection[a]

Nanoparticles	Assay format [a]	Detection system[b]	Linear range/ cells mL^{-1}	Limit of detection/ cells mL^{-1}	Ref.
Au	Direct	colorimetric	CEM: 6.6×10^2-1.3×10^5	300	30
Au	ACNPs	fluoresence	CEM: 5×10^3-2×10^5	1250	31
Au	Enzyme-linked	DPV	K562: 5×10^4-1×10^7	1.0×10^4	32
Chitosan/carbon nanofiber	Electrodeposition	Impedance	K562: 5×10^3-5×10^7	1.0×10^3	33
Carbonnanotubes	cytosensor	DPV	BGC: 1×10^3-1×10^7	620	34
CdTe	Self-assembled monolayer	ASV	K562: 1×10^2-1×10^7	-[c]	35
Au/CuS/MNPs[d]	ACMNP & dual-amplification	FI-CL (Cu^{2+} and Fe^{3+} synergistic reaction system)	Ramos: 80-10000	56	

[a] ACNPs: aptamer-conjugated nanoparticles; ACMNPs: aptamer-conjugated magnetic nanoparticles.

[b] DPV: differential pulse voltammetry; ASV: anodic stripping voltammetry; FI-CL: flow injection chemiluminescence.

[c] Do not reported in their paper.

[d] This method

Mixed sample assays

The FI-CL responses of the target cells with and without mixing with the CEM control cells were also detected. As seen in **Fig. S10**, the CL signals of mixed samples were only slightly higher than those of the pure Ramos target cell samples. Thus, while in some forms of analysis, the nonspecific binding of a small amount of nanoparticles could cause the generation of a false positive signal, the nonspecific extraction of the control cells in this assay could be ingored based on the CL intensity.

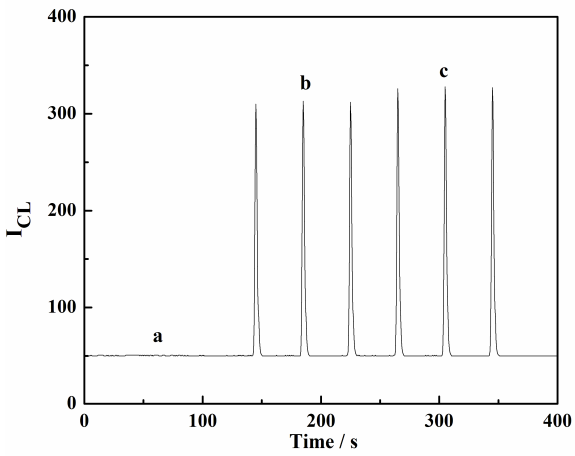

Fig. S10 SECL signals of (a) blank sample, (b) pure target samples, and (c) target cells mixing with the control cells. Both concentrations of target cells and control cells are 2000 cells mL^{-1}.

Blood sample assays

Table S5 SECL signals of blood samples with and without standard Romas target cells

Sample	Blood sample (cells mL^{-1})	Added target cells (cells mL^{-1})	Detected cells (cells mL^{-1})	Recovery (%)
1	-[a]	100	81	81.0
2	-	1000	962	96.2
3	-	10000	9856	98.6

[a] No FI-CL response

Notes and references

1 A. Ambrosi, M. T. Castañeda, A. J. Killard, M. R. Smyth, S. Alegret, A. Merkoci, *Anal. Chem.*, 2007, **79**, 5232-5240.

2 C.-H. Liu, Z.-P. Li, B.-A. Du, X.-R. Duan, Y.-C. Wang, *Anal. Chem.*, 2006, **78**, 3738-3744.

3 A. W. Paton, J. C. Paton, *J. Clin. Microbiol.*, 2005, **43**, 2944-2947.

4 R. Y. Lai, E. T. Lagally, S. H. Lee, H. T. Soh, K. W. Plaxco, A. J. Heeger, *Proc. Natl. Acad. Sci. U.S.A.*, 2006, **103**, 4017-4021.

5 S. K. Poddar, *Mol. Cell. Probes*, 2000, **14**, 25-32.

6 G. Liu, Y. Wan, V. Gau, J. Zhang, L. Wang, S. Song, C. Fan, *J. Am. Chem. Soc.*, 2008, **130**, 6820-6825.

7 S. Zhang, H. Zhong, C. Ding, *Anal. Chem.*, 2008, **80**, 7206-7212.

8 S. Bi, H. Zhou, S. Zhang, *Chem. Commun.*, 2009, **37**, 5567-5569.

9 R. Elghnian, J. J. Storhoff, R. C. Mucic, R. L. Letsinger, C. A. Mirkin, *Science*, 1997, **277**, 1078-1081.

10 D. Li, Y. Yan, A. Wieckowska, I. Willner, *Chem. Commun.*, 2007, **34**, 3544-3546.

11 K. Sato, K. Hosokawa, M. Maeda, *J. Am. Chem. Soc.*, 2003, **125**, 8102-8103.

12 R. C. Bailey, J. M. Nam, C. A. Mirkin, J. T. Hupp, *J. Am. Chem. Soc.*, 2003, **125**, 13541-13547.

13 L. He, M. D. Musick, S. R. Nicewarner, F. G. Salinas, S. J. Benkovic, M. J. Natan, C. D. Keating, *J. Am. Chem. Soc.*, 2000, **122**, 9071-9077.

14 J. Wang, D. Xu, A.-N. Kawde, R. Polsky, *Anal. Chem.*, 2001, **73**, 5576-5581.

15 J. Zhang, S. P. Song, L. H. Wang, H. P. Wu, D. Pan, C. H. Fan, *J. Am.Chem. Soc.*, 2006, **128**, 8575-8580.

16 J. J. Storhoff, S. S. Marla, P. Bao, S. Hagenow, H. Mehta, A. Lucas, V. Garimella, T. Patno, W. Buckingham, W. Cork, U. R. Muller, *Biosens. Bioelectron.*, 2004, **19**, 875-883.

17 T. A. Taton, C. A. Mirkin, R. L. Letsinger, *Science*, 2000, **289**, 1757-1760.

18 Y. W. C. Cao, R. Jin, C. A. Mirkin, *Science*, 2002, **297**, 1536-1540.

19 S. J. Park, T. A. Taton, C. A. Mirkin, *Science*, 2002, **295**, 1503-1506.

20 J. Wang, R. Polsky, D. Xu, *Langmuir*, 2001, **17**, 5739-5741.

21 H. Cai, Y. Xu, N. Zhu, P. He, Y. Fang, *Analyst*, 2002, **127**, 803-808.

22 C. H. Liu, Z. P. Li, B. A. Du, X. R. Duan, *Anal. Chem.*, 2006, **78**, 3738-3744.

23 C. F. Ding, H. Zhong, S. S. Zhang, *Biosen. Bioelectro.*, 2008, **23**, 1314-1318.

24 J. Wang, G. Liu, A. Merkoci, *J. Am. Chem. Soc.*, 2003, **125**, 3214-3215.

25 D. Gerion, F. Q. Chen, B. Kannan, A. H. Fu, W. J. Parak, D. J. Chen, A. Majumdar, A. P. Alivisatos, *Anal. Chem.*, 2003, **75**, 4766-4772.

26 F. Patolsky, A. Lichtenstein, I. Willner, *Angew. Chem. Int. Ed.*, 2000, **39**, 940-943.

27 X. L. Zhang, L. L. Li, L. Li, J. Chen, G. Z. Zou, Z. K. Si, R. J. Wen, *Anal. Chem.*, 2009, **81**, 1826-1832.

28 J. Wang, R. Polsky, A. Merkoci, K. L. Turner, *Langmuir*, 2003, **19**, 989-991

29 J. M. Nam, S. I. Stoeva, C. A. Mirkin, *J. Am. Chem. Soc.*, 2004, **126**, 5932-5933.

30 C. D. Medley, J. E. Smith, Z. Tang, Y. Wu, S. Bamrungsap, W. Tan, *Anal. Chem.*, 2008, **80**, 1067-1072.

31 J. E. Smith, C. D. Medley, Z. Tang, D. Shangguan, C. Lofton, W. Tan, *Anal. Chem.*, 2007, **79**, 3075-3082.

32 D. Du,; H. X. Ju, X. J. Zhang, J. Chen, J. Cai, H. Y. Chen, *Biochemistry*, 2005, **44**, 11539-11545.

33 C. Hao, L. Ding, X. Zhang, H. Ju, *Anal. Chem.*, 2007, **79**, 4442-4447.

34 W. Cheng, L. Ding, J. Lei, S. Ding, H. Ju, *Anal. Chem.*, 2008, **80**, 3867-3872.

35 L. Ding, W. Cheng, X, J. Wang, S. J. Ding, H. X. Ju, *J. Am. Chem. Soc.*, 2008, **130**, 7224-7225.